River Flow 2010 - Dittrich, Koll, Aberle & Geisenhainer (eds) - © 2010 Bundesanstalt für Wasserbau ISBN 978-3-939230-00-7

Simulation of flow in an open channel bend of strong curvature using Detached Eddy Simulation

G. Constantinescu
Civil and Environmental Engineering Department, The University of Iowa, Iowa City, Iowa, USA

M. Koken
Civil Engineering Department, Middle East Technical University, Ankara, Turkey

J. Zeng
Operation and Data Management Division, South Florida Water Management District, West Palm Beach, Florida, USA

ABSTRACT: Understanding the mechanisms through which the momentum and Reynolds stresses are redistributed in strongly curved bends is directly relevant for flow in natural river configurations. In this paper, Detached Eddy Simulation (DES) is used to calculate the flow and turbulence structure in a single open channel 193^0 bend of very high curvature for which the ratio between the mean curvature and the channel width is close to 1.3. For these conditions, the strength of the cross-stream motions and anisotropic effects are very important. This makes it a very tough test case for numerical models. The three-dimensional velocity distributions predicted by DES are compared to the data obtained from an experiment conducted at EPFL-Lausanne. Results show that DES satisfactory capture the distribution of the streamwise velocity in the mean flow and, more important, the distribution of the streamwise vorticity in relevant cross-sections. Comparison with Reynolds Averaged Navier Stokes (RANS) simulations shows that DES is significantly more successful in predicting the velocity redistribution in the channel as a result of the non-linear interactions between the main flow and the cross flow induced by the channel curvature. The success of DES is particularly important, as this technique can be used to conduct numerical simulations at Reynolds numbers close to those present in the field, thus allowing the study of scale effects.

Keywords: Numerical Simulations, Curved Bends, Open Channels

1 INTRODUCTION

Natural rivers are seldom straight over distances larger than a few channel widths. The secondary flow and associated cross-stream circulation in the curved and meandering regions play an important role in the transport processes (e.g., sediment, contaminants).

The flow, sediment transport and associated bathymetry evolution in curved channels are determined to a large degree by the helical motion of the water due to the action of the centrifugal forces present in regions of relatively high channel curvature. In the region close to the outer bank, the shear stress is strongly amplified in the downstream part of the curved region, and some distance past it, before the flow and shear stress distributions recover toward the values associated with straight open channels. Near the bed, sediment particles move toward the inner bank where, eventually, they deposit and raise the bed level by forming a point bar. Concomitantly, the mean flow velocity and bed shear stress increase in the region close to the outer bend where erosion is initiated and a pool is created. As the scour develops at the outer region of the bend, the transversal slope increases until the force induced by the secondary current (main cross-stream circulation cell) against the transversal slope is balanced by the (downwards) component of the gravitational force acting on the sediment particle in the same direction (e.g., Odgaard 1981). At this point equilibrium is reached and the large-scale features of the bathymetry do not change significantly in time. Hence, the cross-stream circulation indirectly determines the flow field by shaping the bathymetry.

In recent years, several fully 3D computations of flow and sediment transport in loose-bed open channels have been performed for bends of moderate curvature for which the ratio between the radius of curvature of the bend, R, and the channel width, B, was larger than 4 (e.g., Wu et al., 2000, Khosronejad et al., 2007, Zeng et al., 2008b). In

all these studies, one or two equation isotropic Reynolds Averaged Navier Stokes (RANS) models were used to account for turbulence effects.

Zeng et al. (2008a) were the first to report 3D RANS simulations with movable bed and with fixed deformed bed corresponding to equilibrium conditions in a very sharp open channel bend (R/B=1.3). The test case (Blanckaert, 2002) was designed to include all processes occurring in the natural river environment in an exaggerated way, in order to make them better visible and to allow validation of 3D morphodynamic models by means of an extremely severe test case.

Comparison of the results of these two RANS simulations with experimental measurements performed at equilibrium scour conditions by Blanckaert (2002) showed that discrepancies between measurements and RANS predictions were due both to failure of the flow module of the morphodynamic code to predict the flow and turbulence structure in the bend and to deficiencies in the modelling of the sediment transport which determines the evolution of the bed. This means that to increase the accuracy of numerical models used to predict flow, sediment transport and morphodynamic changes in loose-bed open channels and natural streams, more complex sediment transport (in particular, bed-load transport) models and more complex turbulence models have to be used.

Even for flat bed conditions corresponding to the initiation of the scour and deposition process, there is wide agreement that to qualitatively and quantitatively capture the intricate cross-stream flow pattern in the curved bend (e.g., the formation of the outer bank cell of cross-stream circulation), an advanced turbulence model capable of accurately resolving turbulence anisotropy effects and the kinetic energy transfer between mean flow and turbulence is needed (e.g., see Blanckaert & de Vriend, 2004, 2005).

Among the options available to increase the accuracy of the predictions of the mean flow and turbulence structure in curved open channels and natural streams are useing anisotropic Reynolds stress RANS models, Large Eddy Simulation (LES), or hybrid RANS-LES approaches. As our long term goal is to be able to use the same numerical model to study flow and sediment transport in natural streams at field conditions, the use of a hybrid RANS-LES model that allows performing eddy resolving simulations at field channel Reynolds numbers (e.g., around 10^6) appears the best option. This is because well-resolved LES is too expensive to simulate the flow at such high Reynolds numbers, while standard LES with wall functions uses a much more simplified approach to account for the processes in the near-bed region and for wall roughness effects compared to an advanced hybrid RANS-LES model like Detached Eddy Simulation (DES).

The present study uses DES (e.g., see Constantinescu & Squires, 2004 for a more detailed discussion of the model) to investigate the flow and turbulence structure in open channel bends of high curvature. The good performance of DES in predicting massively separated flows and junction flows (e.g., flow past bridge piers, bridge abutments, groynes, etc.) over a wide range of Reynolds numbers, in particular compared to RANS, was already proven (e.g., see Constantinescu et al., 2003, Chang et al., 2007, Koken & Constantinescu, 2009, Kirkil et al., 2009, Kirkil & Constantinescu, 2009). However, flow in curved bends do not automatically fall into this category, especially if large emerged / submerged islands or hydraulic structures (e.g., groynes installed to protect against bank erosion) are not present. Thus, a careful assessment of the performances of DES for this type of flows is needed.

One should also mention that, once validated, DES can be a powerful technique to study flow in natural streams not only compared to other numerical approaches, but also compared to experiment. Though in many regards the ideal way to go, detailed field studies of flow in natural river bends are relatively scarce (e.g., Thorne et al., 1985) because of the high costs involved. Moreover, changing conditions in the river during the measurement period adds another level of complexity that has to be taken into account when analyzing the data and using it for validation of numerical models. The resolution at which the measurements are performed within the area of interest in such field studies and the accuracy of these measurements are lower than those of state-of-the-art laboratory experiments. Such experiments conducted in controlled environments allow a detailed investigation of the mean flow and turbulence structure (e.g., Blanckaert, 2002). Still, in many cases such experimental investigations also report detailed measurements only in one or few cross sections which are not enough to exactly determine the position and strength of the large-scale coherent structures in the flow. Such measurements do not allow to accurately estimate the distribution of the friction velocity at the bed and the sidewalls, nor that of the pressure root mean square (rms) fluctuations. This is a serious shortcoming, as the entrainment of sediment particles is driven by the local values of the bed friction and the pressure rms fluctuations. On the other hand, most of the detailed experimental investigations of flow and sediment transport in curved open channels were conducted at channel Reynolds numbers less than, or around, 10^5. A main

question is to what extent the findings from these detailed experimental investigations apply in the field, where the Reynolds numbers can be much larger than 10^6. Investigation of scale effects using DES can help answer some of these questions.

While in the case of a flat-bed curved channel, one can argue that the use of LES (e.g., van Balen et al., 2009) or hybrid RANS-LES approaches should result in more accurate predictions of the flow and turbulence compared to RANS because of the importance of turbulence anisotropy effects, in the case of a more complex bathymetry the answer is not so obvious as most of the secondary motions are primarily pressure driven. This is however an essential question, as after the initial stages of the scour process, the bathymetry features start playing an important role in the redistribution of the mean flow and the formation of shear layers and secondary large-scale vortices. Moreover, natural streams have always a deformed bed. If switching from RANS to a hybrid RANS-LES model will result in a significant improvement of the mean flow and turbulence structure in the open channel at all, or most, stages of its evolution toward equilibrium, then one can argue that the use of such eddy resolving models in codes that have the capability to predict sediment transport and the bathymetry should be undertaken. Better predictions of the mean flow and turbulence will result in a more accurate prediction of the bed shear stresses and of the other quantities that are used to estimate the suspended and the bed load transport and, ultimately, the channel bathymetry.

2 NUMERICAL METHOD, DESCRIPTION OF THE TEST CASE AND SIMULATION SET UP

A general description of the DES code is given in Chang et al. (2007). One should also mention the RANS version of the same code was used by Zeng et al. (2008b, 2010) to calculate flow and sediment transport in similar curved open channels with movable bed, including in the geometry considered in the present paper (Zeng et al., 2008a). The results section details the comparison between the present DES simulation and the corresponding RANS simulation conducted by Zeng et al. (2008b) with a deformed fixed bed.

The 3D incompressible Navier-Stokes equations are integrated using a fully-implicit fractional-step method. The governing equations are transformed to generalized curvilinear coordinates on a non-staggered grid. The convective terms in the momentum equations are discretized using a blend of fifth-order accurate upwind biased scheme and second-order central scheme. All other terms in the momentum and pressure-Poisson equations are approximated using second-order central differences. The discrete momentum (predictor step) and turbulence model equations are integrated in pseudo-time using alternate direction implicit (ADI) approximate factorization scheme. The Spalart-Allmaras (SA) one-equation model was used as the base model in DES and to perform the RANS simulation. Time integration in the DES code is done using a double time-stepping algorithm. The time discretization is second order accurate. Validation of the DES code for flow in channels with bottom mounted cavities and flow past surface mounted bridge piers is discussed in Chang et al., (2007) and Kirkil and Constantinescu (2009).

Figure 1 shows a sketch of the flume in which the *M89* mobile bed experiment was carried by Blanckaert (2002). The flume consisted of three sections: a 9 m long straight inflow channel reach followed by a 193º bend with constant centerline radius of curvature R=1.7 m and a 5 m long straight outflow reach. The total length of the flume was 22.7 m along the centerline. The width of the flume was B=1.3 m and the sidewalls (banks) were vertical. The bed was covered with quasi-uniform sand with an average diameter of about d_{50}=2mm. The bathymetry was measured after the flow and sediment transport reached equilibrium. Also detailed velocity measurements of the flow at equilibrium conditions by means of an Acoustic Doppler Velocity Profiler are available in representative sections for validation (for more details see Zeng et al., 2008a). The inflow discharge was 0.089 m^3/s. The Reynolds number and the Froude number calculated using the flume-averaged flow depth and the flume-averaged velocity were 68,400 and 0.41, respectively.

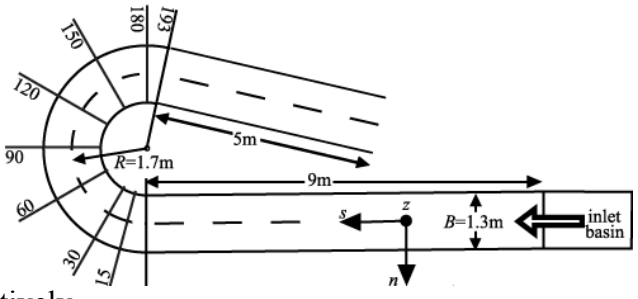

Figure 1 Sketch of the flume in which the experiment was conducted.

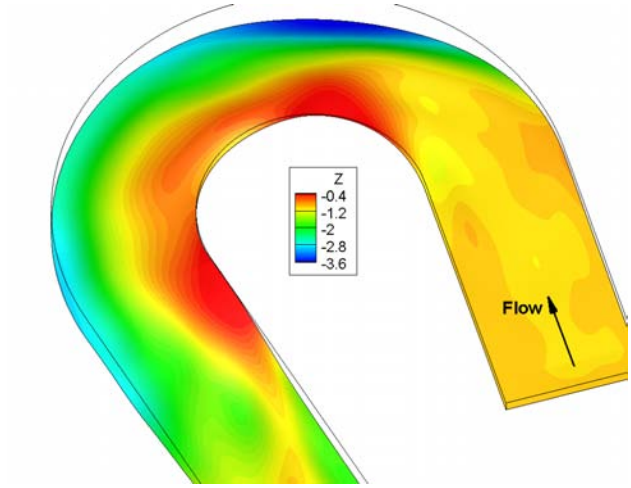

Figure 2. 3D view of the bathymetry at equilibrium conditions. The bed elevation is measured with respect to the mean position of the free surface (z/D=0) in the inlet.

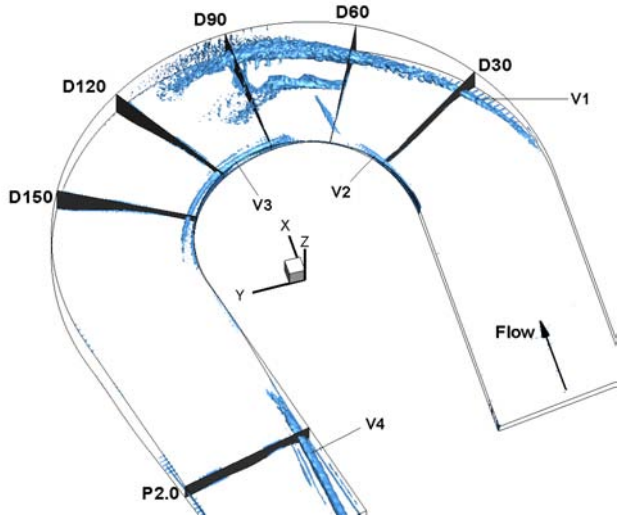

Figure 3. Visualization of the vortical structure of the mean flow predicted by DES using the Q criterion.

The results are presented in non-dimensional form. The length scale is selected to be D=0.115 m. The velocity scale is U=0.61 m/s.

At the inflow section, turbulent inflow conditions corresponding to fully-developed turbulent channel flow with resolved turbulent fluctuations are applied in DES. A steady fully developed precalculated RANS solution was used to specify the inflow conditions in the RANS simulations. At the outflow, a convective boundary condition is used in DES. The free surface is treated as a rigid lid but the free surface deformation measured in the experiment was taken into account when the computational domain and mesh were generated. All the walls are treated as no-slip boundaries. In both RANS and DES, the equivalent total bed roughness estimated using the procedure described in Zeng et al. (2008a) was 0.037 m. This value is comparable with the measured height (0.03 – 0.05 m) of the small-scale traveling dunes observed over the whole bed in the experiment.

The computational domain in DES was meshed using about 10 million cells. The mesh in the RANS simulation was much coarser, but the RANS solution was checked to be grid independent. In both RANS and DES, a minimum grid spacing of one wall unit was used in the wall normal direction to avoid the use of wall functions. The location of the inflow section in DES and RANS was the same (9 m upstream of the bend entrance).

3 ANALYSYS OF MEAN FLOW FIELD AND COMPARISON WITH EXPERIMENT

The bathymetry at equilibrium conditions is depicted in Fig. 2. The measured equilibrium bathymetry shows that scour in the outer half of the cross-section develops upon entering the bend. The flow depth reaches a maximum of about 3*D* in the cross-section situated at 60° within the bend (D60 in Figs. 1 and 3), before reducing to a value of about 2.2*D* in sections D120 and D150. Scour increases again upon approaching the bend exit. The flow reaches a depth of about 2.6*H* in section D180. Then, the scour decays in the straight outflow reach and the bed is about flat in the outer part of section P2.9 (Fig. 1), situated 2.9 m downstream of the end of the curved reach.

As discussed by Zeng et al. (2008a), the rapid development of the transverse bed slope past section D30 induces a rapid spanwise redistribution of the discharge. For example, in section D60 more than 90% of the discharge flows through the outer half of the cross-section and the maximum unit discharge is about three times higher than in the straight approach flow. The shallow inner half of the cross-section over the point bar developing between sections D30 and P1.5 is a kind of dead water zone. Downstream of section D60, about 75% of the flow discharge is conveyed through the outer half of the cross-section. The spanwise distribution of streamwise unit discharge is modulated by the bed topography. Its non-uniformity decreases from section D60 to section D120, and increases again towards the bend exit. In the downstream part of the straight outflow reach, the flow tends to become uniform over the width.

The Q criterion was used in Fig. 3 to visualize the main large-scale eddies present in the mean flow based on DES predictions. The vortex V1 corresponds to the main cell of cross-stream circulation developing on the outer half of the cross section, starting close to the entrance into the bend region. The eddy present close to the channel centerline between sections D60 and D90 corresponds to the shear layer forming on the outer side of the point bar centered around section D75. The dominant vorticity component into that eddy is vertical rather than streamwise. Additionally,

three more streamwise oriented vortices denoted V2, V3 and V4 form in the vicinity of the inner wall and slowly diverge from the inner bank as one move downstream. These three vortices are not connected. Their circulation increases fast downstream of the streamwise position where they originate and then decays slowly in the streamwise direction. Certainly, the presence of a deeper region very close to the inner bank in some parts of the flume favors the formation of these vortices, in particular V3 and V4. One can also argue that the formation of the large-scale eddies triggers the changes in the bathymetry observed at equilibrium conditions close to the inner bank. We are in the process of running a similar simulation with flat bed to try to understand to what degree the formation of these streamwise oriented vortices at the inner bank is dependent on the presence of a deformed bed. As the discussion of the mean flow structure in representative cross section will show, some of these vortices (e.g., V3) can be quite strong. Coupled with the fact that a large amplification of the turbulent kinetic energy is present inside the cores of some of these vortices, it is possible that their formation may substantially amplify the bed friction velocity and pressure fluctuations on the solid surfaces (inner bank, bed) situated in their vicinity.

Figure 4 compares the RANS and DES predictions of the non-dimensional streamwise vorticity in section D60. This section cuts through the main cell of cross-stream motion, denoted V1. Similar to the experiment, DES captures the formation of a relatively circular patch of high streamwise vorticity at the end of the bottom attached boundary layer induced by the cross stream motions in the vicinity of the bed over the inner half of the section. This compact patch of high streamwise vorticity corresponds exactly to the position of the core of V1 as visualized by the Q isosurface in Fig. 3. Meanwhile, RANS does not capture the presence of a clear region that can be associated with V1. In fact, when the Q criterion is used to visualize the main eddies in the RANS solution, the strength of V1 is significantly underpredicted compared to DES. Moreover, the distribution of the streamwise velocity in the same section (not shown) is also affected. The presence of a strong vortex centered around $\eta/D=3.5$ in section D60 induces the formation of a tongue of higher streamwise velocity in the vicinity of the bed, over the outer half of the section, in the experiment and DES solution. This redistribution of the streamwise velocity due to the presence of a strong compact vortex (V1) is not captured by RANS. One should also mention that in the experiment and DES the core of V1 corresponds to a region where the streamwise velocity is smaller than that in the surrounding flow. As one moves downstream of D90, the core of V1 increases while its strength diminishes rapidly.

Next, we focus our attention on section D120 (Fig. 5). At this streamwise location the main recirculation eddy is still present. No compact core of strong streamwise vorticity is present at this section. However, both the experiment and DES show the presence of a relatively large patch of stronger streamwise vorticity compared to that in the surrounding flow. This patch is situated close to the free surface and the outer wall. Consistent with the underestimation of the strength and compactness of the vorticity distribution inside the core of V1 at section D60, no patch of vorticity corresponding to V1 is present in section D120.

Meanwhile, a strong vortex V3 is present close to the inner bank in DES. This vortex is clearly visible in Fig. 5. Unfortunately, no velocity measurements were available in that region. However, the presence of a strong vortex at the inner bank is fully consistent with the local scour observed close to the inner bank ($\eta/D<-4$). Moreover, the vorticity levels between $\eta/D<-2$ and $\eta/D=-4.5$ are in very good agreement in experiment and DES. Away from the bed, RANS predicts significantly lower vorticity values in this region. One should mention that 2D streamline patterns show the presence of an eddy similar to V3 in the RANS simulation. However, its strength is couple of times lower compared to DES that also shows a very large amplification of the turbulent kinetic energy in the region where the core of V3 is located. A strong vortex is needed to induce local scour, especially that the streamwise velocity (see Fig. 6) in the same region is relatively low, both in RANS and DES.

Comparison of the streamwise velocity distributions in Fig. 6 shows other interesting differences between RANS and DES predictions. The core of large streamwise velocities already started moving toward the inner bank. Experimental measurements show that the center of the core is situated close to the centerline in section D120 and the patch containing relatively high values of the streamwise velocity penetrates up to $\eta/D\sim-3.5$ on the inner side and up to $\eta/D\sim3$ on the outer side of the section. Though some differences are observed between the experiment and DES, the overall agreement is quite satisfactory. The RANS distribution of the streamwise velocity presents several qualitative and quantitative differences with both experiment and DES. The peak values inside the core of large streamwise velocities are smaller. However, the area occupied by this patch is larger. In particular, rather than extending up to $\eta/D\sim3$ on the outer side of the section, the core penetrates in the lower part of the section until close to the

outer bank. This penetration is possible because of the severe underprediction of the coherence of V1 in the same section.

Next, the streamwise velocity distributions in section P2.9 situated in the downstream straight reach of the flume are compared in Fig. 7. Though RANS predictions are closer to DES in terms of the overall level of agreement with experiment, some differences can still be pointed out. The position of the region of very high streamwise velocity is situated too close to the inner wall and the peak values are overestimated in RANS. Though that is also true in DES, the differences with the experiment are smaller. However, most of the important differences in the flow structure in section P2.9 between DES and RANS are related to the differences in the distributions of the streamwise vorticity in the two simulations.

RANS totally fails to predict the circular region of negative vorticity associated with V4 (see Fig. 3) at $\eta/D\sim-4.5$ and the tongue of negative vorticity starting at the crest of the hump centered around $\eta/D=0$. Both these features are present in the streamwise vorticity distributions calculated based on velocity measurements. Moreover, the vorticity levels in the two regions of negative vorticity are comparable in DES and experiment. By contrast, in RANS the streamwise vorticity values are very low in that section. Inspection of the 2D streamline patterns shows that even in RANS a recirculation region in predicted close to the bed, in between the inner wall and $\eta/D=-0.5$. However, the circulation is very close to zero and the presence of a strong vortex (V4) and a weaker cell centered at $\eta/D=-2.5$ is not captured. The 2D streamline patterns in experiment and DES are very similar in this region. The strength of V4 is so large that it induces the formation of a bottom attached vortex that, at times, ejects patches of positive vorticity. This is the main mechanism that modulates the intensity of V4 in the instantaneous flow fields. This detaching boundary layer is situated too close to the bed to be accurately captured by the experimental measurements. The formation of V4 can also provide part of the explanation why the water elevation becomes larger near the inner wall downstream of P1.0. As V4 moves away from the inner wall (Fig. 3) and starts loosing its coherence, one expects the differences in the bathymetry levels would gradually diminish.

4 CONCLUSIONS

The present study considered the flow in an open channel bend of very high curvature over realistic topography corresponding to equilibrium scour conditions. For this test case, that greatly challenges the predictive capabilities of the numerical solver and turbulence model, the flow and turbulent structure are controlled by the non-linear interaction between the downstream velocity and the cross-stream circulation. This interaction is further complicated by interaction with the bathymetry, which leaves a strong fingerprint on all characteristics of the flow field.

DES revealed several strong streamweise oriented vortices formed near the inner bank. The presence of these vortices generally results in a strong amplification of the turbulence (velocity and pressure fluctuations) close to the solid boundaries situated in the vicinity of these flow structures (e.g., inner bank, channel bed). The strength and exact extent of some of these vortices were not possible to estimate from experiment because of the lack of data near the two sidewalls.
Results clearly show that compared to RANS, DES is able to better capture the distribution of the streamwise velocity and streamwise vorticity that is a direct measure of the strength of the secondary flow over the strongly curved bend. A better prediction of these two variables will automatically result into a better prediction of the streamwise and cross-stream components of the bed friction velocity and of the depth averaged horizontal velocity components that are used by the sediment transport module in codes that have the capability to predict the bed deformation.

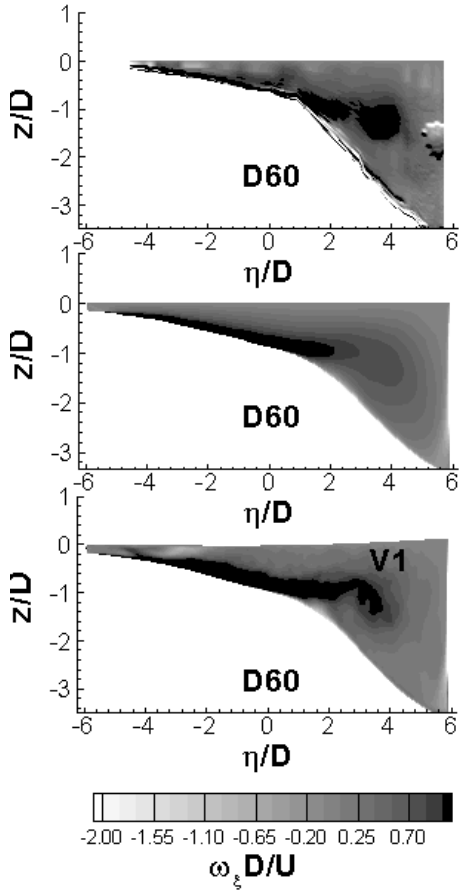

Figure 4. Mean flow streamwise vorticity ω_ζ(D/U) in section D60. a) experiment; b) RANS; c) DES.

The data generated from DES simulations will be used to enhance insight in the physics of the flow in bends of strong curvature over flat and equilibrium bathymetry and to study scale effects between the range of Reynolds numbers art which most experimental studies are conducted and the range of Reynolds numbers typically encountered in the field. These simulations will allow enlarging the range of geometrical and flow parameters over which detailed information on the flow physics, streamwise variation of the strength of the secondary flow and integral parameters characterizing the flow in curved bends are available.

REFERENCES

Blanckaert, K. 2002. Flow and turbulence in sharp open-channel bends. PhD-thesis Nr 2545, Ecole Polytechnique Fédérale Lausanne, Switzerland.

Blanckaert, K., de Vriend, H. J. (2004). Secondary flow in sharp open-channel bends. Journal of Fluid Mechanics, 498, 353-380.

Blanckaert, K., de Vriend, H. J. 2005. "Turbulence structure in sharp open-channel bends." Journal of Fluid Mechanics, 536, 27-48.

Chang, K., Constantinescu, G., Park, S.O. 2007. Assessment of predictive capabilities of Detached Eddy Simulation to simulate flow and mass transport past open cavities. ASME J. Fluids Engineering, 129(11), 1372-1383.

Constantinescu, G., Chapelet, M.C., and Squires, K.D. 2003. Turbulence modeling applied to flow over a sphere, AIAA Journal, 41(9), 1733-1743.

Constantinescu, G., Squires, K.D. 2004. Numerical investigation of the flow over a sphere in the subcritical and supercritical regimes. Physics of Fluids, 16(5), 1449-1466. DOI 1070-6631/2004/16(5)/1449/18.

Kirkil, G., Constantinescu, G., Ettema, R. 2009. DES investigation of turbulence and sediment transport at a circular pier with scour hole. J. Hydraulic Engineering, 135(11), 888-901.

Kirkil, G., Constantinescu, G. 2009. Nature of flow and turbulence structure around an in-stream vertical plate in a shallow channel and the implications for sediment erosion. Water Resources Research, 45, W06412.

Koken, M., Constantinescu, G. 2009. An investigation of the dynamics of coherent structures in a turbulent channel flow with a vertical sidewall obstruction. Physics of Fluids, 21, 085104, DOI 10.1063/1.3207859.

Khosronejad, A., Rennie, C., Neyshabouri, S., Townsend, R.D. 2007. 3D numerical modeling of flow and sediment transport in laboratory channel bends. J. Hydraulic Engineering, 133(10), 1123-1134.

Odgaard, A.J. 1981. Transverse bed slope in alluvial channel bends. Journal of the Hydraulics Division, ASCE, 107(12), 1677-1694.

Thorne, C, Zevenbergen, L., Pitlick, J., Bradley, J., Julien, P. 1985 Direct measurements of secondary currents in a meandering sand-bed river, Nature, 315, 746-747

Van Balen, W, Uijttewaal, W. And Blanckaert, K. 2009 Large eddy simulation of mildly curved open channel flow. J. Fluid Mechanics, 630, 413-442.

Wu, W., Rodi, W., Wenka, T. 2000. 3D numerical modeling of flow and sediment transport in open channels. J. Hydraulic Engineering, 126(1), 4-15.

Zeng, J., Constantinescu, G., Blanckaert, K. and Weber, L. 2008a, Flow and bathymetry in sharp open-channel bends: Experiments and predictions, Water Resources Research, 44, W09401, doi:10.1029/2007WR006303.

Zeng, J., Constantinescu, S.G. and Weber, L. 2008b, A 3D non-hydrostatic model to predict flow and sediment transport in loose-bed channel bends, IAHR J. of Hydraulic Research, 46(3).

Zeng, J., Constantinescu, S.G. and Weber, L. 2010, 3D calculations of equilibrium conditions in loose-bed open channels with significant suspended sediment load, J. Hydraulic Engineering, in press

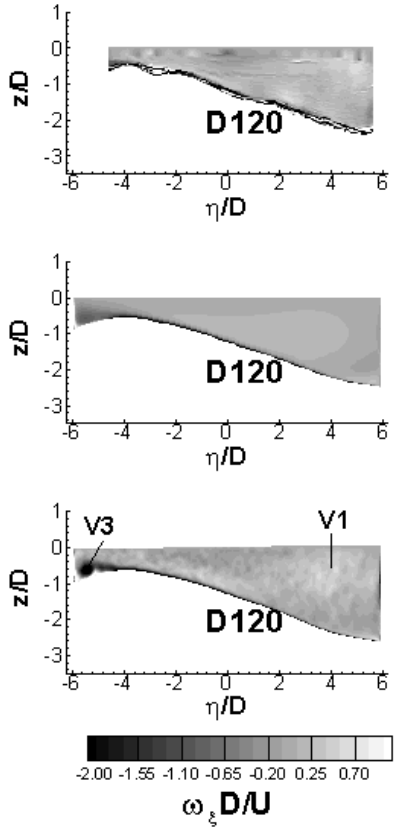

Figure 5. Mean flow streamwise vorticity ω_ξ(D/U) in section D120. a) experiment; b) RANS; c) DES.

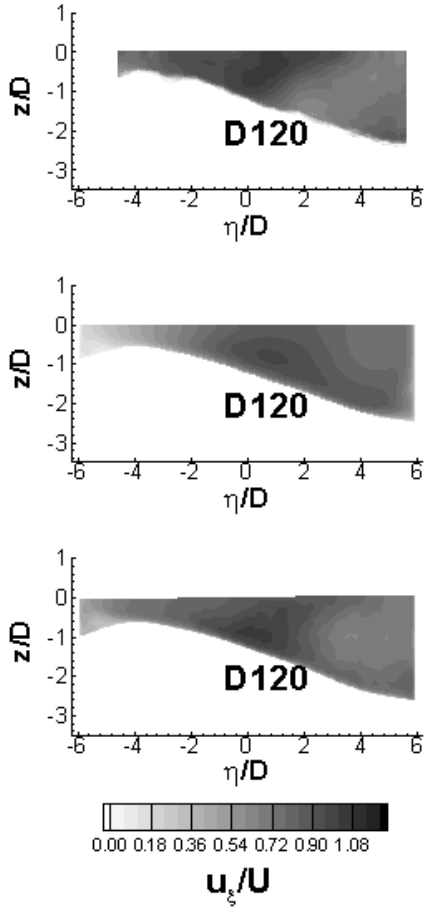

Figure 6 Mean flow streamwise velocity, υξ/U, in section D120. a) experiment; b) RANS; c) DES.

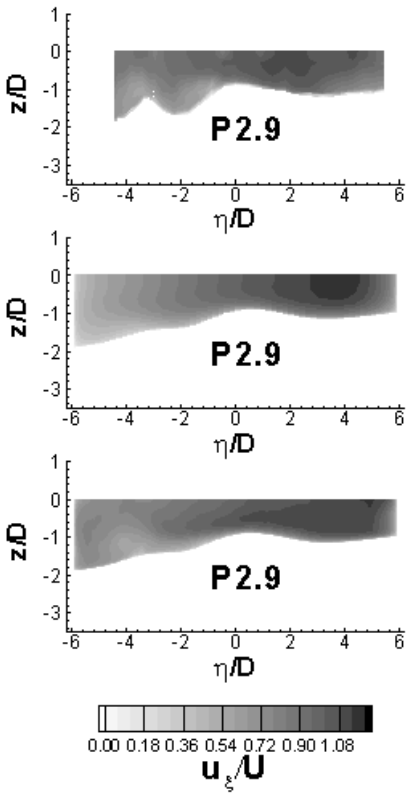

Figure 7 Mean flow streamwise velocity, υξ/U, in section P2.9. a) experiment; b) RANS; c) DES.

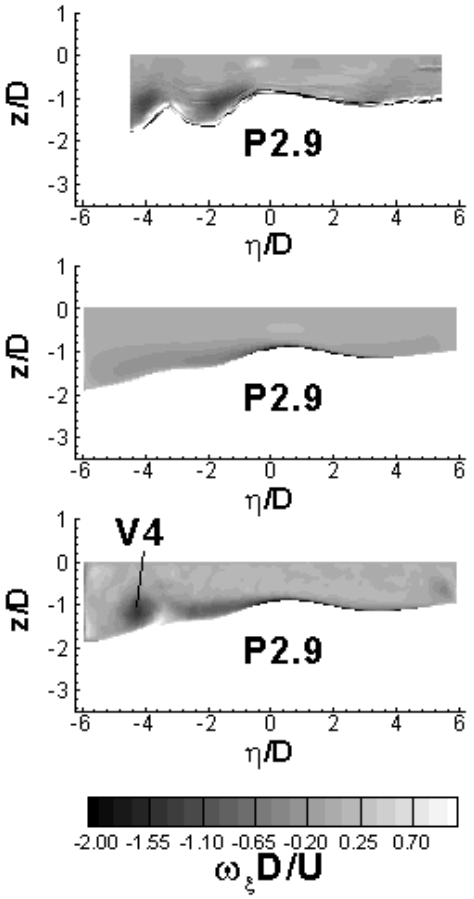

Figure 8. Mean flow streamwise vorticity ω_ξ(D/U) in section P2.9. a) experiment; b) RANS; c) DES.